Bedform Response to Flow Variability

J.M. Nelson, B.L. Logan & P.J. Kinzel
US Geological Survey, Golden, CO, USA

Y. Shimizu
University of Hokkaido, Sapporo, Japan

S. Giri
Delft Hydraulics, Delft, The Netherlands

R.L. Shreve
University of Washington, Seattle, WA, USA

S.R. McLean
University of California, Santa Barbara, CA, USA

ABSTRACT: Laboratory observations and computational results for the response of bedform fields to rapid variations in discharge are compared and discussed. The simple case considered here begins with a relatively low discharge over a flat bed on which bedforms are initiated, followed by a short period with double the original discharge during which the morphology of the bedforms adjusts, followed in turn by a relatively long period of the original low discharge. For the grain size and hydraulic conditions selected, the Froude number remains subcritical during the experiment, and sediment moves predominantly as bedload. Observations show rapid development of quasi-two-dimensional bedforms during the initial period of low flow with increasing wavelength and height over the initial low-flow period. When the flow increases, the bedforms rapidly increase in wavelength and height, as expected from other empirical results. When the flow decreases back to the original discharge, the height of the bedforms decreases in response rapidly, but the wavelength decreases much more slowly. Computational results for the same conditions simulate the formation and initial growth of the bedforms fairly accurately, and also predict an increase in dimensions during the high-flow period. However, the computational model predicts a much slower rate of wavelength increase, and performs less accurately during the final low-flow period, where the wavelength remains essentially constant, rather than decreasing. In addition, the numerical results show less variability in bedform wavelength and height than the measured values. Based on observations, these discrepancies may result from the simplified model for sediment particle step lengths used in the computational approach. Assuming a constant value for the step length neglects the role of flow alterations in the bedload sediment-transport process, which appears to result in predicted bedform wavelength changes smaller than those observed.

1 INTRODUCTION

The greatest barrier to using computational models for predicting flood inundation, sediment transport, and large-scale morphologic change in rivers is the presence of bedforms and their complex adjustment to temporally varying flow fields. Even the very best computational flow models in rivers rely heavily on accurate specification of local roughness for making correct predictions, and local roughness is frequently dominated by form drag on bedforms that vary significantly in space and time. Typically, this roughness is parameterized using empirical approaches which have been developed based on constant discharges; the evolution of bedforms and the drag they generate is poorly understood in flows with strong temporal variability in flow discharge. Improving the current capability for predicting flow and sediment transport in natural rivers with varying hydrographs requires an improved capability for predicting the spatially distributed adjustment of the bedform fields to variations in discharge.

Over the past two decades, improvements in the methods for measuring and visualizing flows over bedforms have driven data collection efforts in the laboratory and in field situations; these measurements have greatly improved understanding of those flows. This work has clarified certain aspects of the basic bedform instability mechanism, and has also provided accurate basic data on mean flow and turbulence fields for a variety of flow conditions and bedform shapes and sizes for testing computational flow models. Currently, there are several computational codes that have been shown to yield reasonable predictions of the complex flow structure over bedforms using both direct-numerical simulation techniques and turbulence closure methods. There are also coupled models in which tested flow models have been combined with sediment-transport models in order to investigate the initiation and morphologic evolution of bedforms, notably the recently-

published models developed by Giri & Shimizu (2006) and Niemann & Fredsøe (in press). With continued verification and refinement, these approaches and others like them will provide the capability needed for predicting the initiation and behavior of bedforms in constant flows, and for predicting the adjustment of bedforms to temporally varying flows.

In this short paper, results from the computational model for bedform initiation and evolution developed by Giri & Shimizu (2006) are compared to laboratory experimental data for bedforms developing and adjusting to a simple time-varying flow. This model, which has also been discussed and compared to flow data by Nelson et al. (2005), and Giri & Shimizu (2006), uses a two-dimensional closure-type flow model (described in more detail below) in combination with a probabilistic model for bedload sediment "pick-up" and deposition and an advection-diffusion model for suspended-sediment transport. The approach has been shown to yield good results for the development and morphology of bedforms in constant flows, although with some discrepancies (see Giri & Shimizu, 2006).

The goal of the research presented herein is to assess this state-of-the-art method for making predictions of bedform behavior in time-varying flows, and to try to identify aspects of the problem that need further research to develop this and similar methods into practical predictive tools for scientists and engineers. Verified methodologies for predicting evolution of the bedform field in rivers appear to be a very real possibility in the near future, and are likely to dramatically improve the current capabilities for predicting river behavior across a range of temporal and spatial scales.

2 LABORATORY EXPERIMENTS

The laboratory experiments consisted of observations of bedform initiation and growth on an initially flat bed for a simple time-varying discharge. The experiments were carried out in the sediment transport research flume at the U.S. Geological Survey's Geomorphology and Sediment Transport Laboratory (GSTL) in Golden, Colorado. This tiltable flume has a test section approximately 6m in length, with a width of 0.25m and maximum depth of approximately 0.40m. Flow is controlled via two pumps, one of which has a variable frequency control to allow accurate discharge variation. Discharge is determined within 0.5% using an inline vortex flowmeter. Typically, the initial bed for the experimental runs was constructed by adjusting the flume to a specified slope and screeding the sediment bed to that same slope using the flume rails as a reference. This process was checked using both laser surveys and still water to assess accuracy; typically slopes can be set accurately to within 0.0001.

The sediment used for the experiments described here was well-rounded, well-sorted 0.6-mm filter sand. Bearing in mind the range of depth and discharge in the flume, the sediment size was chosen to mutually satisfy the various competing requirements of excellent grain visibility for photography, high Rouse number, subcritical Froude number, low relative roughness, high particle Reynolds number, and expected bedform characteristics. Bedform phase diagrams from Middleton & Southard (1984) were used in this assessment, with conditions chosen to correspond principally to 2-dimensional bedforms based on their empirical data. Giri & Shimizu. (2006) used finer sand (0.28mm) in their earlier work and used a very narrow flume (0.10m) to enforce two-dimensionality. Experiments at GSTL showed that the 0.28mm size used with the discharge per unit width used in the experiments carried out in the narrow flume actually results in three-dimensional bedforms in the 0.25m-wide flume at GSTL, in agreement with bedform phase diagrams. For these experiments, one of the questions to be addressed concerned the importance of three-dimensional processes, particularly with regard to how these processes might affect the variability of the bedform dimensions, so it was undesirable to force two dimensionality through the flume dimensions.

Measurements were carried out during the bedform evolution runs using a variety of noninvasive techniques. For the runs discussed in this paper, time-lapse videography was used to record the evolution of the bed, and direct measurements of wavelengths, heights, and water depths were also made during the runs. For some runs, laser-Doppler velocimetry (LDV) and high-speed videography were also employed to obtain detailed near-bed flow statistics along with grain motion information at various collocated positions along the bedforms. In some cases, particle image velocimetry data were collected

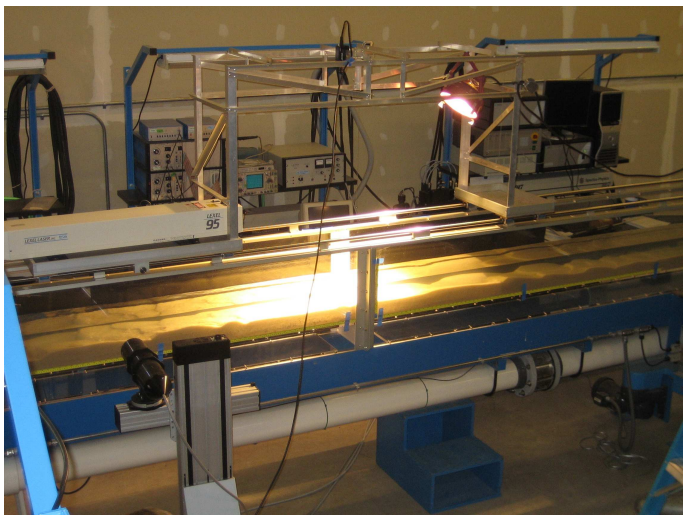

Figure 1. Photograph of the lab test section and measurement equipment.

to corroborate and extend the record obtained using LDV measurements. In this short paper, the focus is on the observed geometric characteristics of the bedforms, although some justification and discussion of the other measurements is offered below. The flume and other laboratory details are shown during an experimental run in the photograph in Figure 1.

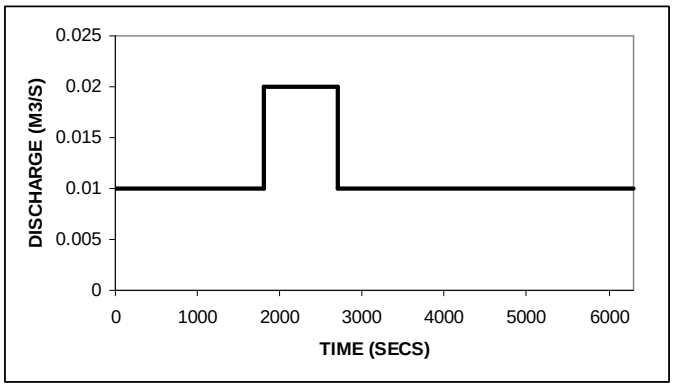

Figure 2. Hydrograph used in bedform evolution experiments.

The hydrograph used for most of the measurement program was chosen to be the simplest one that contained both a sharp rise and a sharp decrease in discharge, as shown in Figure 2. The initial bed slope of the flume was set to 0.002 for all the runs shown here. This value was chosen to provide an initial average bed stress equal to about three or four times the critical shear stress for the sediment. This combination results in rapid initial formation of bedforms while keeping the Froude number low and the Rouse number high (very little suspended sediment).

3 NUMERICAL MODELING

The details of the numerical approach used to predict the results of the bedform evolutions are discussed fully in papers by Giri & Shimizu (2006, 2007) and Giri et al. (2006) and will not be repeated in this short paper. However, some brief comments to indicate how the components of the model function are worthwhile.

3.1 The Flow Model

The flow model is based on the solution of the two-dimensional Reynolds-averaged Navier-Stokes equations cast in a boundary-fitted coordinate system. The coordinate system is updated at each time step of the morphologic evolution predictions. The turbulent momentum fluxes are treated using a nonlinear k-ε closure; although the advantages of this approach over a standard k- ε are modest, the nonlinear treatment is apparently more accurate for treating separation zones. Nelson et al. (2005) compared this flow model to a direct-numerical simulation (DNS) model and found that predictions for the mean flow compared to measured data about as well as the DNS approach, but that the DNS approach performed slightly better for turbulence quantities. For practical grid sizes, neither the closure model nor the DNS were very accurate for turbulence structure near the bed and in the shear layer immediately downstream of the bedform crest due to the importance of neglected small-scale turbulence. The DNS approach was deemed impractical for morphologic evolution due to the need to compute the flow solution iteratively. The DNS solution required more than an order of magnitude greater computation time for similar grid spacings. Tjerry & Fredsøe (2005) and Niemann & Fredsøe (in press) used a k-ω closure for their model of flow over dunes, and appeared to achieve similar levels of accuracy in predicting detailed LDV measurements. Nelson et al. (2005) also showed that the model used in this paper predicted near-bed pressure distributions accurately, which is a key part of predicting the structure of the flow due to the importance of form drag.

Boundary conditions for the flow model were a no-slip condition at the bed, a kinematic condition at the free surface, and a periodic boundary condition on the streamwise model domain. Computations were performed for various model domain lengths and results were found to be insensitive to this condition provided that the domain was several times larger than the length of the largest bedform modeled, as one might expect. Solutions were found by splitting the equations into non-advective and purely advective components, solving the non-advective phase with a central difference method and successive over-relaxation for pressure, and solving the advection phase using a high-order Godunov scheme known as the cubic-interpolated polynomial (CIP) method. Solutions found using this approach have been compared to measurements and the model has been shown to be fairly accurate for predicting flow over bedforms (Nelson et al., 2005; Giri & Shimizu, 2006).

3.2 The Sediment-Transport Model

In order to make realistic predictions of the behavior of bedforms, bedload transport predictions need to go beyond relating local time-averaged flow quantities, like boundary shear stress, to local transport. As shown by several linear instability analyses for bedforms, the basic instability giving rise to bedforms is related to the fact that a bump on a bed under a turbulent shear flow produces the highest velocity (at a fixed distance from the bed) and bed stress upstream of the crest of that bump, a point originally made by Benjamin (1959) in the context of wind flow over waves. Thus, if transport is related to near bed velocity or stress, the maximum sediment flux is upstream

of the bump, and deposition must occur between that maximum and the crest: the bump grows. Inserting this physical model into a simple linear stability analysis yields the fact that all wavelengths grow and the shorter the wavelength, the faster it grows; a fastest growing wavelength is not identified. Over the past few decades, several ideas have been put forth to explain this result and provide for the selection of a fastest-growing wavelength on an initially flat bed. These include the role of gravity in altering sediment motion, the scale over which turbulence responds to shear in the flow, and a spatial lag produced by the shift between the local flow conditions and the local transport associated with the grain by grain transport process. Although each of these effects may play some role, these authors believe that observations suggest that the last of these three is most important. In simple terms, if the shift in stress upstream of the bump crest is significantly shorter than the distance sediment particles move, it will not produce deposition on the bedform crest. Following this argument to its logical conclusion yields the idea that initial ripple lengths on flat beds should be proportional to sediment grain size, since the length of saltation trajectories scale roughly with grain size, thereby defining a lower wavelength cutoff below which the features cannot form (i.e. when the saltation lengths are greater than the flow-induced upstream shift in maximum stress). Including these physical effects requires the use of a disequilibrium approach for bed load transport, much as treating suspended sediment in nonuniform flows requires the use of an advection-diffusion model.

For the calculations presented here, the disequilibrium bedload-transport model presented by Nakagawa and Tsujimoto (1980) was employed. Their approach specifically separates entrainment of sediment (so-called "pick-up") and the distrainment (or deposition rate) of sediment. In their model, the dimensionless entrainment rate is given by

$$p_s \sqrt{d/(\rho_s/\rho - 1)g} = 0.03\tau_*(1 - 0.035/\tau_*)^3$$

where p_s is the sediment entrainment rate, ρ and ρ_s are the fluid and sediment density, and τ_* is the dimensionless shear stress. The distrainment rate is given by

$$p_d = p_s f_s(s)$$

where $f_s(s)$ is a probability density function of sediment particle step length given by Nakagawa and Tsujimoto (1980) as

$$f_s(s) = \frac{1}{\Lambda}\exp\left(-\frac{s}{\Lambda}\right)$$

where Λ is the mean step length and s is the distance from the point of entrainment. Based on a few experimental studies and on theoretical considerations, Λ is typically assumed proportional to sediment grain size (D) for bedload transport, with the constant of proportionality dependent to some degree on the flow characteristics. The value of Λ is set to 20D for the results presented here.

In a recent study, Giri & Shimizu (2007) showed that, as might be expected, the detailed results of the bedform evolution model are sensitive to the value of Λ. Although outside of the scope of this short paper, one of the primary reasons for the experimental program described here was to make accurate determinations of this poorly constrained quantity using high-speed videography.

The actual manner of application of the sediment-transport model above is to use bed stresses inferred from velocities computed at the closest grid point to the bed assuming a logarithmic velocity profile and an appropriate grain roughness. This is somewhat confusing, as the quantity thus derived is NOT the boundary shear stress in either a time-averaged or instantaneous sense, but some surrogate developed from an instantaneous velocity. Nevertheless, this allows variability from the flow model to enter the sediment-transport field, thereby introducing appropriate small-scale perturbation to the bed that could not be treated using some time or ensemble-averaged quantity. The method also allows for variations in flow structure to alter the net sediment flux; two time series of near-bed velocity with the same mean but significantly different variances yield significantly different sediment fluxes due the nonlinear dependence on velocity in the equation for sediment entrainment given above. Based on experiments on flow and sediment transport over bedforms and downstream of backward-facing steps, capturing this variability appears to be important for understanding bedform behavior (Nelson et al., 2005). Thus, even though the model for bedload transport used here in relatively simple, it appears to capture the important physical processes necessary for modeling bedform initiation and evolution.

4 RESULTS

4.1 Experimental Observations

In Figure 3a-d, video frames of the bed morphology are shown for 4 times during the hydrograph shown in Figure 2. Figure 3a, shows the bed about 5 minutes after the beginning of the experiment, when a

complete train of bedforms was first present over the test section. Before this time, the bed surface showed incomplete individual ripples with an initial length of about 0.08-0.09m; over time these features grew and additional features formed until a complete train of bedforms was observed. The average wavelength of the features once a complete train of bedforms was present was approximately 0.1m; these bedforms were quite two-dimensional, with continuous crests across the width of the flume and only minor variations in the position of the crest line on the order of 0.01m. Over the remainder of the initial low flow period, bedform heights increased to about 0.02m and wavelengths increased up to about 0.2-0.25m, with a considerable amount of variability in both measures. Figure 3b shows the bedform morphology after 1800s, at the end of the initial low-flow period. Water depth during this flow varied only by 1-2 mm and averaged 0.09m.

charge at 2700s, the immediate response of the bedforms was a rapid decrease in height (flattening), without much change in wavelength. Much smaller amplitude bedforms formed on the flattened upper stoss side of the original features, resulting in a rather confusing combination of long, relatively high features mantled with a few lower, shorter features.

In most cases, the shorter features migrated up to the crest of the large ones without much effect, but in some cases the smaller features interacted strongly with the larger crests, resulting in much more three-dimensional structure with oblique crests and crests with bifurcated crest lines. Over time, this interaction resulted in shorter average features, but the process was relatively slow and showed significant variability. The final bedform morphology at the end of the hydrograph is shown in Figure 3d. In order to quantify the variability, the hydrograph shown in Figure 2 was run three times on an initially flat bed.

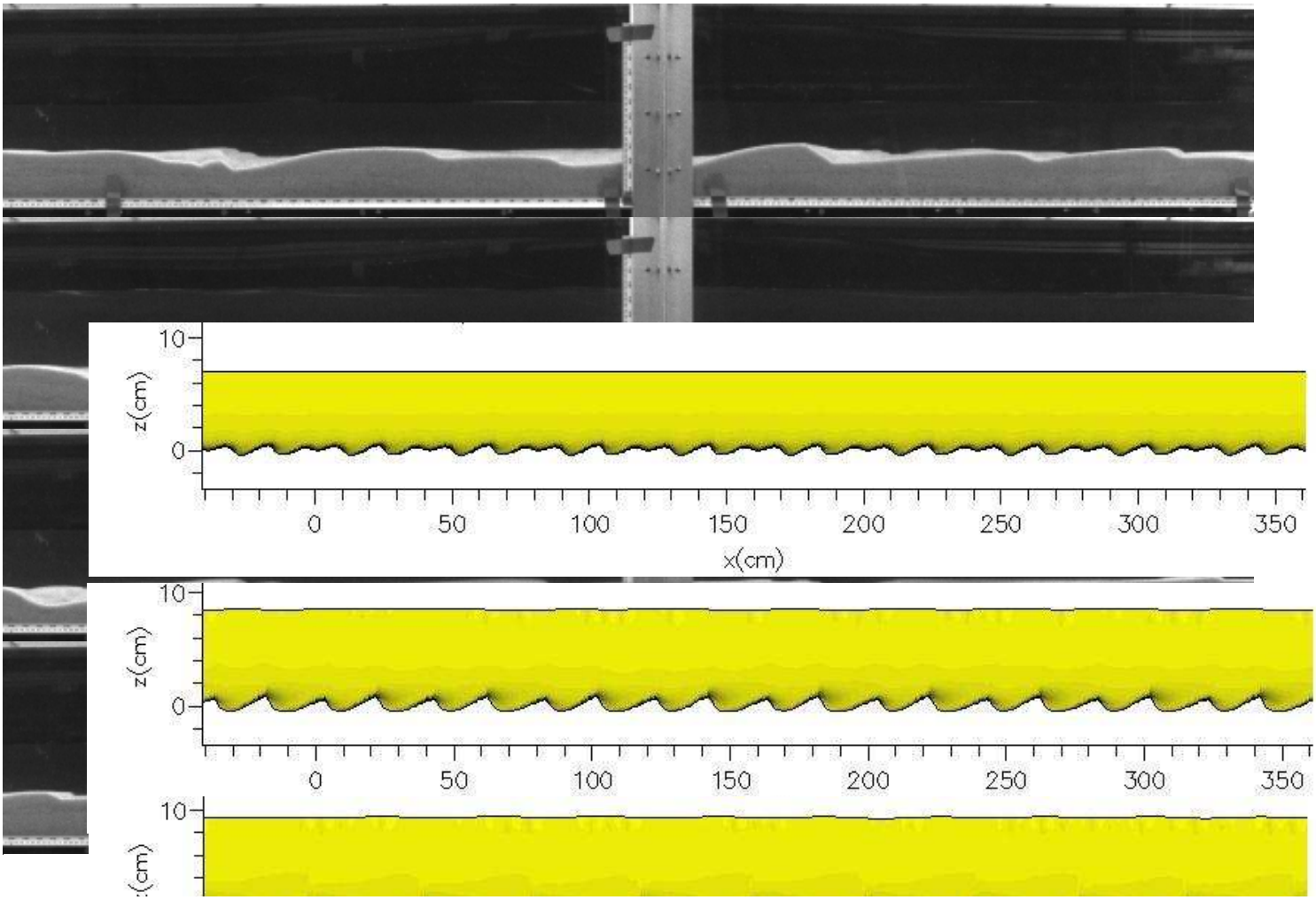

Figure 4. (a) top, computed bed for T=300s, (b) T=1800s, (c) T=2700s, (d) bottom, T=6300s

Whe
the bed
height
respect
the hig
water i
period
increas
catchin
forms.

ferent scales and vertical exaggeration of a factor of five, which should be borne in mind when comparing Figures 3 and 4. In the computational results, the initial wavelength shown in Figure 4a is about 20% longer than that found in the experimental observations. By the end of the low flow period, the wavelengths and heights are very close to the same for the experimental and laboratory runs. During the high flow period, the computational results show increasing wavelength and height, although to a lesser degree than that seen in the experiments.

After the period of high flow, the heights of the bedforms decrease slightly in the computational results, although only by about 20%, much less than that seen in the experimental measurements. More noticeably, the computational results predict very little change in wavelength when the flow drops; there is no evidence that the wavelength decreases. This may be partially due to the fact that the experimental results show a markedly smaller increase in wavelength during the high flow period, such that the wavelength at the end of that period of the hydrograph is similar to that found for the experimental results after the final period of low flow. However, it is also plausible that the model is not capable of capturing the processes leading to the decreasing wavelength seen in the laboratory observations.

1 5 DISCUSSION

In order to understand the discrepancy between the model and the observations for the high flow period, two additional hydrographs were run. First, the low discharge was applied to an initially flat bed for the entire flow period, and second, the high-flow section of the hydrograph was moved to the beginning of the flow period, such that the high flow (q=0.02 m^3/s) occurred for the first 900s of the bed evolution, followed by the low flow for the remainder of the experiment. The major discrepancy between the modeled and the measured bedform morphology appears to be an underprediction of the increase in wavelength during the high flow period; it seems plausible that the underestimate of the bedform height may principally be a byproduct of the lack of wavelength change, since bedform steepnesses fall in a relatively narrow range for the case of bedload transport. It would be unreasonable to expect the model to predict the correct height for bedforms that are about half as long. Looking at these other flow scenarios and the associated wavelength evolution provides more information on to what degree the bed configuration seen at the end of the runs are what the low flow alone might produce, and whether the timing of the high flow period makes a significant difference in the final morphology.

In Figure 5, the wavelength evolution for the original runs (with standard deviations) is shown with the model results and for the cases of constant low flow and earlier high flow. Interestingly, both the model and the lab results for all the hydrographs produce similar results at the end of the runs, with a wavelength around 0.3-0.5m and heights of about 0.02m. This corroborates the results found by Giri and Shimizu (2006) to some extent, in that the model predicts the observed morphology at the end of a relatively long period of constant flow. However, it also confirms that the approach does not work as well for the case of time-varying flows. The model performs reasonably for the initiation of bedforms on a flat bed and predicts the general evolution of increasing

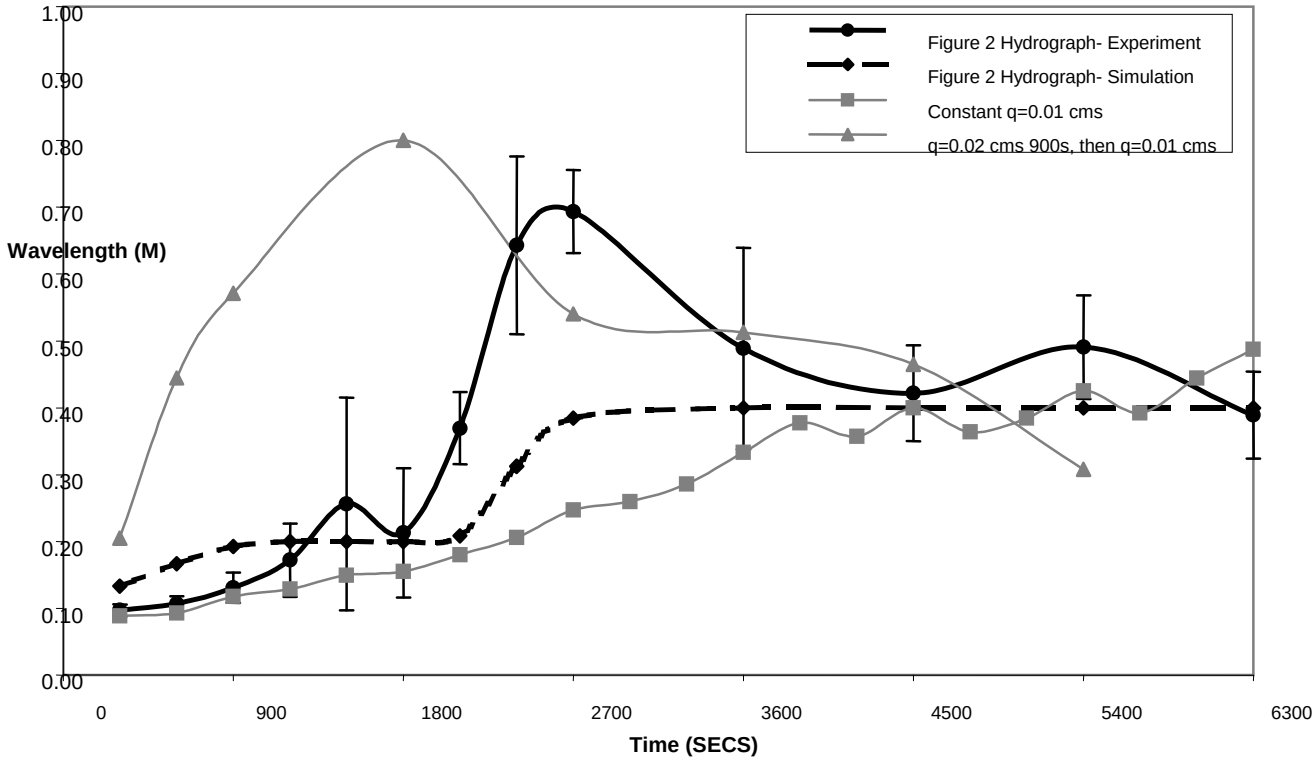

Figure 5. Wavelength evolution for modeled and computed conditions

wavelength and height from that initial stage, but the response to a rapid flow change is muted relative to measurements. As shown in Figure 5, the model results do show a more rapid increase in wavelength during the high-flow period relative to a constant low flow, but the rapid increase and subsequent decrease are not correctly predicted.

There are a variety of physical effects that might produce the observed error. First, if the model overpredicted the form drag at the onset of high flow, such that the sediment flux was underpredicted, the evolution would take place slower than expected. However, as shown in Figure 6, the ratio of total to skin friction stress behaves reasonably; the skin friction increases by about a factor of 2 when the discharge increases and then decreases somewhat as the form drag increases. It seems more likely that the wavelength selection process is incorrect in the model, which suggests that the step-length approach may be at fault. When the stress or near-bed velocity increases in that approach, the amount of sediment moved increases, but the average step length between the point of entrainment and the average point of distrainment does not, this is almost certainly an oversimplification of the real situation.

Figure 6. Time history of total versus average skin friction stress for the hydrograph in Figure 2. The dark line corresponds to no form drag, the light trace is the initial low flow and constant high discharge, and the darker trace is the decreasing flow and final low flow period.

As noted above and in Giri and Shimizu (2007) the value of Λ has a significant effect on the wavelength selection. For the runs here and for those presented in earlier tests of the model for constant discharge, a single value appropriate to the "average" flow conditions has been specified. While this appears to be adequate for constant flow, it is likely that the shortcomings of the morphologic evolution model for time-varying flows are associated with this assumption. For the case at hand, where the initial response to the sudden increase in flow is to roughly double the average skin friction, it seems clear that the average step length of particles moving as bedload should also increase in response. This effect would preferentially stop the growth of shorter features while promoting that of longer features. Although it would not necessarily explain all the discrepancy between the predicted and measured wavelengths shown in Figure 5, it seems that the effect of a more general approach for step length would certainly move the results in the correct direction.

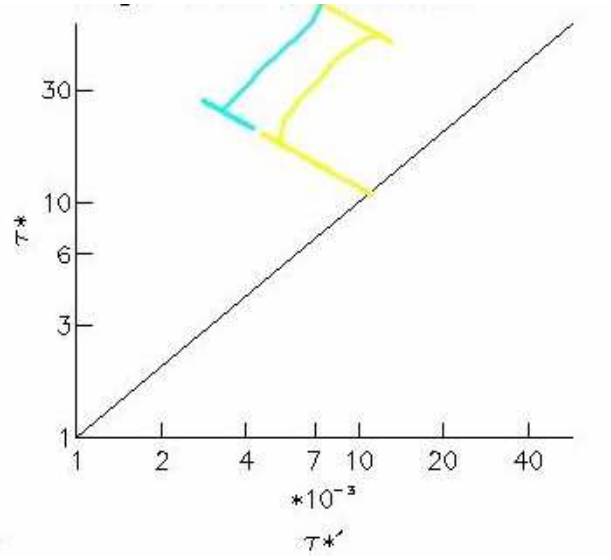

6 CONCLUSIONS

The next step in the iterative process between laboratory and field measurements and computational model development appears to lie in the measurement and detailed characterization of the bedload sediment particle step length. As noted above, high-speed videography combined with LDV measurements are currently be used to address this issue. At this point, flow models appear sufficiently accurate to address the morphological evolution of bedforms, and predictions for relatively constant conditions are encouraging. For the first time, sediment-transport models for bedforms are taking direct consideration of the effects of variability in predicting sediment motion and the subtle feedback between the flow and topographically induced accelerations that govern the local turbulence fields and, thereby, the transport of sediment. Continuing progress on this problem requires a better-defined relation between the details of particle motion and near-bed flow, particularly including the concept of step length and its precise determination over a wide range of flow conditions. Engineers and scientists working in this area are extremely close to truly predictive models of bedform behavior. These approaches seem likely to revolutionize the current ability to predict flow and morphologic behavior in rivers.

7 REFERENCES

Benjamin, T.B. (1959) Shearing flow over a wavy boundary, *J. Fluid Mech* ,6, 161-205.

Giri, S., S. Yamaguchi, Y.Shimizu, and J.M. Nelson (2006), Simulating temporal response of bedform characteristics to varying flows, RCEM.

Giri, S., and Y. Shimizu (2006), Numerical computation of sand dune migration with free surface, *Water Resour. Res. 42*, W10422, doi:10.1029/2005WR004588.

Giri, S., and Y. Shimizu (2007), Validation of a numerical model for flow and bedform dynamics, *Ann. J. of Hydraul. Eng*., JSCE 51, 139144.

Middleton, G.V., and J.B. Southard (1984), Mechanics of Sediment Movement, S.E.P.M. Short Course 3, Society of Economic Paleontologists and Mineralogists, 401 pp.

Nakagawa, H., and T. Tsujimoto (1980), Sand bed instability due to bedload motion, *J. Hyd.Div.*, ASCE 106, 2029-2051.

Nelson, J.M., A.R. Burman, Y. Shimizu, S.R. McLean, R.L. Shreve, and M.W. Schmeeckle (2005), Computing flow and sediment transport over bedforms, Proceedings of the 4th IAHR Symposium on River, Coastal and Estuarine Morphodynamics, IAHR, Urbana, Ill.

Niemann, S., and J. Fredsøe (in press), Sand dunes in unidirectional flow, *Journal of Hydraulic Engineering*.

Tjerry, S., and J. Fredsøe (2005), Calculation of dune morphology, *J. Geophysical Res.*,110, F04013, doi: 10.1029/ 2004JF000171.

Acknowledgements: Research work reported in this paper was supported by the US Geological Survey National Research Program, NSF grant CTS-0120135 to S.R. McLean and J.M. Nelson, and NSF grant EAR-0125525 to R.L. Shreve and J.M. Nelson, and the Japan Society of Promotion of Science Fellowship 17-05093.